Mater. Res. Soc. Symp. Proc. Vol. 1622 © 2014 Materials Research Society
DOI: 10.1557/opl.2014.74

Nanoprobe Diffusion in Poly(Vinyl-alcohol) Gels and Solutions: Effects of pH and Dehydration

[1]Hacène Boukari, [2]Candida Silva, [2]Ralph Nossal, and [2]Ferenc Horkay

[1]Department of Physics and Engineering, Delaware State University, Dover, DE 19901
[2]*Eunice Kennedy Shriver* National Institute of Child Health and Human Development, National Institutes of Health, Bethesda, MD 20892

ABSTRACT

We report fluorescence correlation spectroscopy (FCS) measurements of the translational diffusion of two fluorescent nanoprobes, rhodamine (R6G) and carboxytetramethylrhodamine (TAMRA), embedded in poly(vinyl alcohol) (PVA) solutions and gels. The diffusion coefficient was measured as a function of the PVA concentration and pH. Furthermore, we designed and built an optical chamber to determine the diffusion coefficient of the nanoprobes within the PVA solutions and gels subjected to controlled dehydration. We find that 1) lowering pH causes an apparent slowing down of the diffusion of the nanoprobes, 2) increase of PVA concentration and crosslink density also induce slowing down of both nanoprobes, and 3) dehydration induces systematic decrease of the diffusion of TAMRA in both solutions and gels. Taken together, these results demonstrate that transient physical interactions between the nanoprobes and the PVA linear polymers have a significant effect upon nanoprobe diffusion.

I. INTRODUCTION

Hydrogels are essential for biomedical applications. Examples of their use are engineering of tissue phantoms, designing extracellular matrices for tissue regeneration, and developing efficient drug delivery systems [1-5]. Understanding their structural and dynamical properties is therefore necessary, especially with the growing demand for hydrogels tailored for specific applications. In particular, the sieving properties of gels remain poorly understood despite numerous investigations at both theoretical and experimental levels. A general consensus on the parameters that control the transmissibility of various materials through the gels has yet to emerge.

Recently, we demonstrated how fluorescence correlation spectroscopy (FCS) could be applied to study the diffusion of various nanoprobes – both small fluorophores and nanoscopic fluorescent biomacromolecules – in polymer solutions and gels [6,7]. We reported FCS measurements of various fluorescent nanoprobes (e.g. BSA, Phycoerythrin, dextran, polystyrene beads) in differing PVA solutions, and showed that the measurements can be analyzed using De Gennes' model [8]. Two relevant length scales, the size of the nanoprobe (d) and the mesh size (ξ) of the host polymer system, were identified. In PVA solutions, when the size of the nanoprobe is comparable to the mesh size of the solution, the dependence of the apparent diffusion coefficient of the nanoprobes on the PVA concentration can be described by a stretched exponential, the exponent being related to the solvent quality [7,9,10]. In PVA gels, we found a strong correlation between the elastic modulus of the gel and the apparent diffusion time of the small fluorescent probe, TAMRA (carboxytetramethylrhodamine) [6].

In this study, we report FCS measurements on the diffusion of a different nanoprobe, rhodamine R6G, in PVA solutions and PVA gels. R6G is a non-reactive, small, water-soluble fluorophore with high quantum yield (excitation/emission: 480/500 nm.) We chose PVA as a model system because this polymer is water-soluble, neutral, optically transparent (both in solution or gel), and stable. Furthermore, various structural properties have been characterized using complementary techniques such as small-angle neutron scattering [11-12]. We investigate the effect of pH on the diffusion of R6G fluorophores in PVA solutions and report FCS measurements on the diffusion of R6G in PVA solutions and gels as a function of the polymer concentration.

We have also designed an optical chamber to probe in-situ changes of the diffusion of fluorescent nanoprobes while PVA solutions and gels are dehydrating slowly via evaporation of water through a porous membrane. With this custom-made, microscope-based FCS setup we monitored changes of the fluorescence of TAMRA samples with time as dehydration occurred. The setup is equipped with two photocount detectors, allowing us to operate the instrument under cross-correlation mode, which is ideal for reducing the effect of afterpulsing. Since the dehydration process was controlled and slow, we collected FCS correlation functions (5-10 min) at half hour intervals during the experiment (7 to 15 hours). Analysis of the correlation functions yield schanges of the nanoprobe concentration from the amplitude of the measured FCS correlation function and changes of the diffusion time of the nanoprobes within the host polymeric samples. Concurrently, changes of the fluorescence, which is related to the changes of concentration of the fluorescent nanoprobes, were used to monitor and calculate changes of the sample volumes.

II. EXPERIMENTAL DETAILS
II.1 SAMPLE PREPARATIONS

II.1a Poly(vinyl-alcohol): For our study, PVA ($M_w \approx$ 85 kDa, Sigma-Aldrich) was dissolved in de-ionized water at 95 ^{o}C and kept at this temperature for several hours. PVA samples were then prepared at room temperature with concentrations ranging from 1% to 8.6% (w/v). Because hydrogen-bond formation tended to induce physical gelation (aging) of PVA solutions, we heated the solutions at 85 ^{o}C for more than 1 hour. The solutions were then let cool to room temperature and measured soon thereafter.

II.1b Nanoprobes: Rhodamine 6G (R6G) (M_W=650 Da) and carboxytetramethylrhodamine (TAMRA, MW=850 Da) were acquired from Invitrogen (Invitrogen, Carlsbad, CA, USA). R6G was shipped in powder form while TAMRA was in solution. Water-based samples of each probe were prepared at relatively high concentration and left on the bench for few days for complete dissolution and mixing. FCS was applied to assess the state of dissolution and stability in water.

II.1c Preparation of PVA solutions and gels: Samples of unlabeled PVA solutions with different PVA concentrations were prepared and vortexed at room temperature. For the FCS measurements, nanomolar concentrations of the fluorescent probes were added to the solutions, and left to stand for several hours for complete mixing to occur. Mixtures whose PVA concentrations exceeded the critical entanglement concentration (~3%) were cross-linked by gludaraldehyde at pH = 2. The crosslink density, [X], was estimated based on the ratio of the glutaraldehyde concentration and that of the PVA. Samples of the mixed solutions were loaded into 40 μl chambers (Grace Bio-Labs, Inc., Bend, Oregon, USA), which have optically-transparent bottom windows made of glass coverslips for FCS. In the case of gels, the mixtures were left at least one hour for complete gelation.

II.1d Chamber for probing nanoprobe diffusion in dehydrating solutions and gels:

We have designed and built an optical chamber to measure the effect of dehydration on nanoprobe diffusion. Figure 1 shows a schematic diagram of the chamber that was attached to the existing FCS setup All parts were custom-made. Unlike an earlier version of the chamber in which we induced osmotic deswelling of the PVA samples by contact with PVP solutions [13], in the present experiment we used a porous membrane (Spectra/Por, Spectrum Labs) with a small molecular weight cut-off (MW~ 3500 Da) which slowed down the evaporation rate. The silicon-rubber spacers were cut from double adhesive

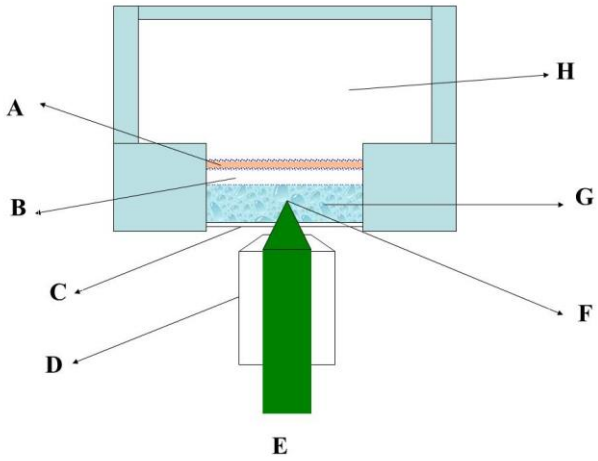

Fig.1: Schematic diagram of the chamber used for measuring changes of the volume of a solution or gel: (A): porous membrane (3500 Da); (B) Air gap ~0.5 mm; (C) cover slip; (D)microscope objective (oil, NA 1.4); (E) Laser beam; (F) Detected volume; (G) sample; (H) Air.

sheets purchased from Grace-Bio-Labs [14].

II.2 Fluorescence Correlation Spectroscopy

II.2.1 FCS Experimental Setup: FCS measurements were performed with a custom-made instrument described in [15] and with a portable FCS unit marketed by Hamamatsu. The custom-made instrument utilizes an inverted microscope (Olympus IX70) with an oil-immersion objective (60X, 1.4 N.A) and confocal collection optics. For fluorescence excitation, a 1.5-mW 543-nm incident HeNe laser beam (Uniphase, San Jose, California, USA) was first expanded and then focused by the objective onto a small spot having a micron to submicron lateral radius. However, only few microWatts of the laser power were used in the experiments in order to reduce photobleaching and excitation of molecular triplet states. The emitted fluorescent beam was collected by the same objective and focused onto an optical fiber (OZ Optics, Carp, Ontario, Canada) that has a small core diameter (< 25 μm diameter). The small diameter of the fiber assures confocal detection necessary for delimiting small volumes of interest. For detection and photocounting, two avalanche photodiodes (SPCM AQ-14, PerkinElmer EG\&G, Vaudreuil, Canada) were used in cross-correlation mode to reduce the effects of detector afterpulsing on the correlation functions, which is especially measurable at short time scales (< 10 μs). The TTL pulses of the photodiodes were processed and correlated by a digital correlator (BI-9000AT, Brookhaven Instruments Corp., Holtsville, New York), generating the intensity-intensity time-correlation functions.

The Hamamatsu FCS unit (model C9413) is equipped with a 473 nm LD-pumped solid-state laser, a high-sensitivity photomultiplier tube with low afterpulsing, a 25 μm diameter pinhole for confocal detection, a water-immersion objective (Olympus UApo 40X W/340; NA=1.15), and a built-in numerical code for correlating the time-sequence of the photocounts. In most measurements, the 1 mW input laser beam was attenuated to 3 μW, and the cut-off wavelength of the high-band emission filter was set to 495 nm. Fitting of the measured correlation functions and calculation of photocounting histograms were performed using a built-in software package provided by Hamamatsu.

II.2.2 Background on FCS: The basic principles of FCS have been described elsewhere [16-20]. Briefly, FCS is an optical technique in which the fluctuations in detected fluorescence can be used to determine details of the intramolecular dynamics (viz. photodynamics) or molecular dynamics of the particles (viz. diffusion). Typically, a laser beam excites fluorescence of particles in a sample, and the emitted fluorescence intensity from a small volume is measured as a function of time. Because of the movement of the particles in and out of the volume or the changes in the photodynamics of the particles, the emitted fluorescence signal fluctuates. In FCS, the fluctuating signal is time-correlated using the following correlation function

$$F(\tau) = 1 + \frac{< \delta I(t) \delta I(t+\tau) >}{< I(t) >^2} \qquad (1)$$

where $\delta I(t) = I(t) - < I(t) >$ denotes the deviation of the intensity $I(t)$ emitted by the fluorescent particles at time t from the average intensity, $<I(t)>$. Analysis of this correlation function can reveal the underlying mechanisms behind the fluctuations. For example, in the case of monodisperse particles diffusing freely in a solution, one can derive the following expression:

$$F(\tau) = 1 + \frac{1}{N}\frac{1}{\left(1+\frac{\tau}{\tau_d}\right)}\frac{1}{\left(1+p\frac{\tau}{\tau_d}\right)^{1/2}} \quad . \qquad (2)$$

Here r_0 and z_0 characterize the ideal Gaussian profile ($W(r,z) = Ae^{-2\left(r/r_0\right)^2} e^{-2\left(z/z_0\right)^2}$) of the focused excitation beam, N denotes the average number of particles in the excitation volume, $p=\left(r_0/z_0\right)^2$ is a constant, and $\tau_d = r_0^2/4D$ is the diffusion time, where D is the translational diffusion coefficient. Moreover, for dilute solutions, the Stokes-Einstein relation, $D = \frac{k_B T}{3\pi\,\eta d_H}$, expresses the diffusion coefficient in terms of the viscosity, η, of the solvent (η = 0.1 centipoise for water), the hydrodynamic diameter of the particles, d_H, the temperature, T (295 K, room temperature), and the Boltzmann constant, k_B = 1.38x10^{-23} J/K. In this latter expression, d_H describes an overall size of the particle with an arbitrary shape; for spherical particles, it is just the diameter of the particles.

Together with the average fluorescence intensity, $<I>$, the amplitude A=*[F(0) -1]* can be obtained from either fitting the measured FCS functions or estimating the amplitude from the limiting value *[F(τ→0)-1]*. The apparent brightness of an individual nanoprobe can be defined by the ratio

$$B = < I > \bullet \mathrm{A} \qquad (3)$$

which, for a fixed intensity of the incident beam, should be independent of the number of the nanoprobes in the solution (since both $<I>$ and $1/A$ are both proportional to the number of the nanoprobes in the detected volume). Given practical considerations such as variations in pipetting and possible binding of the fluorescent molecules to the sample holder, this ratio may be useful when assessing changes of photophysical properties and/or assembly of the nanoprobes in the solution.

III. FCS Measurements and Results

III.1 Effects of pH on the diffusion of R6G in PVA solutions and gels.

In Fig.2 we show the apparent diffusion time of R6G scaled with respect to the diffusion time of R6G in water (pH = 6.5) as a function of PVA concentration at two different values of pH (2.0 and 6.5). The pH was measured with color-sensitive paper indicators. The measurements were collected in PVA solutions. The data indicate

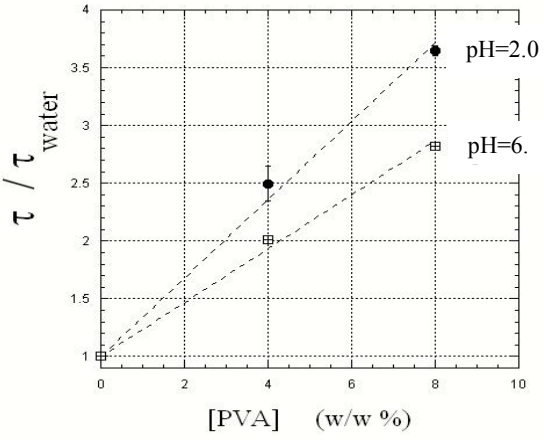

Fig.2: Changes of the diffusion time of R6G in PVA solutions, shown as a function of PVA concentration and pH.

an increase in the diffusion time with decreasing pH, suggesting slowing down of the. Reducing the pH tends to decrease the brightness of R6G, and it was not possible to collect reliable FCS data below pH = 2.

III.2 Effects of Crosslinking of PVA Solutions on R6G Diffusion.

We also measured the diffusion of R6G nanoprobes in gels prepared at different PVA concentrations and crosslinked with gludaldehyde at pH = 2 and at different cross-link densities. The measured correlations of R6G nanoprobes in these gels can be readily fit to Eq.2, yielding the apparent diffusion time. In Fig.3 we plot changes in the apparent diffusion times of R6G nanoprobes moving in gels as a function of PVA concentration and cross-link density. Here, the figure shows two remarkable effects: 1) at a fixed crosslink density, the more concentrated the PVA gel, the slower the diffusion of the nanoprobe, and 2) at constant PVA concentration, the more crosslinked the gel, the slower is the nanoprobe. Similar behavior was observed with TAMRA, whose excitation/emission are in a rather different range (~ 540/560 nm).

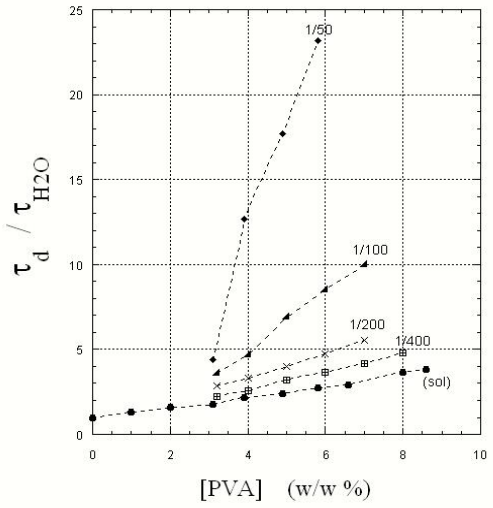

Fig.3: Changes of the apparent diffusion time of R6G fluorophores are plotted as a function of the PVA concentration and cross-link density of the gels (pH=2).

To further assess the dynamical behavior of R6G fluorophores in the gels, we set up an exchange assay in which a gel (volume 200 μl) prepared with [PVA] = 5% and [X] = 1/100 and containing 50 nM concentration of R6G was placed in direct contact with water (1 ml) at room temperature. The gel, which was formed in a small chamber with removable top and was in contact with the bottom glass coverslip of the FCS chamber (see section II.1d), was left to stabilize for one hour. Then, fresh Millipore-grade water (pH=6.5) was added to the top of the gel and the cover of the chamber was closed. Since the gel was initially acidic (pH = 2), we exchanged the water several times until its pH approached 6.5 as measured by paper pH indicators. We monitored in situ changes in the average fluorescence intensity and generated FCS correlation functions of the R6G nanoprobe in the gel during pH change. We noticed that as the pH approached the neutral condition, the average fluorescence intensity increased. Meanwhile, the amplitude of the correlation functions remained constant. This demonstrates that the increase of fluorescence at higher pH is caused by a fast pH exchange (fast outward flux of protons) and slow diffusion of the R6G into the overlaying water. It took about half an hour before we observed a measureable gradual rise of the amplitude of the FCS correlation functions, suggesting reduction in the concentration of the nanoprobes in the gel. Using FCS we verified that the R6G nanoprobes that diffused into the top water appeared free, i.e., unattached to larger structures.

We also performed the inverse exchange, namely the addition of water containing relatively high concentration of R6G to PVA gels prepared with various concentrations and crosslink

densities, but containing low to no R6G nanoprobes. We monitored the rise of the fluorescence intensity, which indicated the diffusion of the nanoprobes into the gel. Further analysis of FCS correlations collected after reaching a steady state of the exchange showed that the diffusion time of the nanoprobes in the gel was similar to that measured in typical gels prepared from solutions that contained the nanoprobes (no-exchange). Remarkably, the diffusion time of the nanoprobes appeared longer than that obtained from corresponding PVA solutions.

III.3 Effects of Dehydration on the Diffusion of TAMRA Nanoprobes in PVA Solutions and Gels

Using the microscope-based FCS instrument, we monitored in-situ changes of the fluorescence intensity of TAMRA nanoprobes while PVA solution and gel samples, in which the fluorescent nanoprobes were embedded, were dehydrating through a porous membrane (see Fig.1 for the chamber). Initially, both the solution and gel contained [PVA]=4% (W/W) and the gel was cross-linked at [X]=1/200. In Fig.4 we plot these changes as a function of time. Note that the fluorescence intensity was scaled with respect to the initial intensity measured before the samples were subjected to dehydration. Two characteristic features of the plots should be highlighted: 1) the increases of the intensities reaching a peak at t_p~7.7 hour for the solution and t_p~15.6 hour for the gel, and 2) the rapid drops of the intensities immediately after.

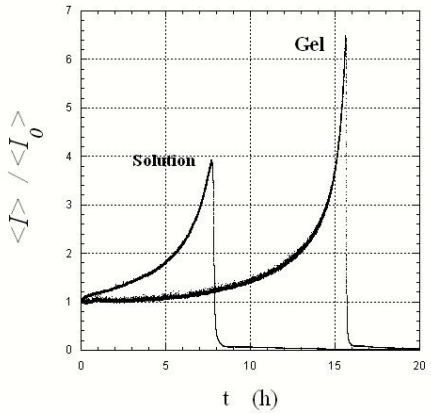

Fig.4: Changes of the measured fluorescence intensity of TAMRA fluorophores are monitored with time as the host PVA solution and gel are continuously dehydrating through evaporation.

For the analysis of the data in Fig.4 we assume that the changes in the intensity result mainly from changes in the average number of fluorophores in the observed volume and that there is no loss of TAMRA during dehydration. Thus, the rising part of the intensity can be attributed to a gradual increase of the concentration of the TAMRA fluorophores as the volume of the solution or gel decreases. The rapid drop of the intensity occurs once the interface between the solution or gel and the air drops below the height of the laser beam (detected volume.) Using Eq.2 we fitted the correlation functions, collected over a 4 to 6 minute period every 30 minutes during the course of dehydration (7 hrs and 15 hrs). The results shown in Fig.5 indicate slowing down of the nanoprobe due to increasein the concentration in both the solution and the gel with time. Note that crosslinking the PVA solution slows the nanoprobe almost twofold. If we assume a one-to-one relation between changes of the fluorescence intensity and those of the volume of the shrinking system, we can re-plot the diffusion time as a function of the concentration of the PVA

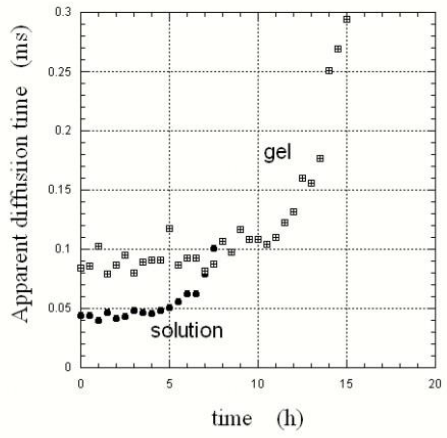

Fig.5: Changes of the apparent diffusion time of TAMRA fluorophores during the dehydration of PVA solution and gel.

solution and gel as shown in Fig.6. That is, $I/I_0 = c/c_0$, where I and c denote, respectively, the values of the fluorescence intensity and the concentration of the PVA; I and c_0 (4 % in our case) describe the initial values of the respective denotations. In this figure, we include changes of the diffusion time of the same nanoprobe measured from PVA samples prepared with corresponding PVA concentration, but not-shrunken.

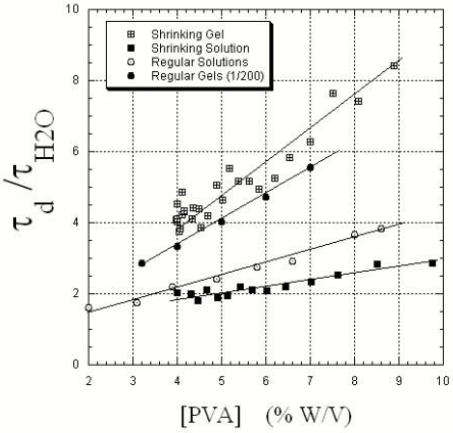

Fig.6: Changes of the measured diffusion time of TAMRA fluorophores are plotted as a function of the PVA concentration of two PVA samples (solution and gel) during dehydration (see text). Also, we include the dependence of the diffusion time of the same nanoprobe measured in samples of solutions and gels prepared at corresponding concentration and cross-link density and without dehydration. The lines are guides to the eyes.

IV. Discussion

FCS has emerged as a powerful tool to measure the translational diffusion of nanoprobes embedded in a host polymer system [6-7,21-23]. Understanding nanoprobe diffusion in polymer systems is rather challenging. Central to this problem is the question of length scales and possible interactions such as hydrodynamic interactions and binding [7,25]. For the case of R6G-PVA samples, one can identify two characteristic length scales: the mesh size of the polymer system (ξ) and the size of the nanoprobe (d). From SANS data collected on samples prepared with PVA solutions and gels we estimate the mesh size to be heterogeneous and lie between 2 and 10 nm in the semi-dilute regime [11,12]. Interestingly, crosslinking appears to have little effect on this mesh size (short length scale) though relative large structures (> 30 nm) are formed. We note that gel-formation occurs about 3% W/V, which can be denoted as the critical concentration. The overall size of R6G and TAMRA nanoprobes used in this study is about 1.6-1.8 nm, which is close to the mesh size of the PVA system. Thus, the changes in the diffusion coefficient shown in Fig.3 cannot be accounted for by the corresponding changes of the viscosity of the host PVA system. Rather, de Gennes' model more adequately describes the data as was previously found [6--8].

Lowering the pH tends to slow down the diffusion of R6G nanoprobes in PVA solutions as shown in Fig.2. It is worth noting that changing the pH does not significantly affect the diffusion of the nanoprobes in solutions in the absence of PVA. Thus, we surmise that the acidic environment enhances either nanoprobe-PVA interactions or PVA-PVA interactions (or both). The nanoprobes contain titratable groups and become more hydrophobic as pH decreases.

It is well-known that at room temperature hydrogen bonds tend to turn PVA solutions into physical gels over time. Based on the observations made on chemically cross-linked gels (see Fig.3) one should expect slowing down of the diffusion of nanoprobes in aging PVA samples. Although not shown in this report, we indeed observed thiseffect in PVA solutions left undisturbed for several months. FCS correlation measurements showed significant increase in the diffusion time of TAMRA nanoprobes in the aged samples.

The pH exchange assays show that the effect of pH on nanoprobe diffusion is reversible as the pH is cycled back and forth between acidic and neutral conditions. The pH effect is observable in gels, even though the PVA chains are partially immobilized. In summary, the nanoprobe-

PVA interaction appears to be affected by the pH; however, these interactions do not create permanent bonds between PVA and the fluorophores, as can be inferred from the exchange assays which show that R6G or TAMRA nanoprobes can diffuse freely in and out of the gels.

As shown in Fig.3, crosslinking of PVA solutions affects the dynamics of R6G fluorophores. In solutions, we found that the more concentrated the solution, the slower the nanoprobes diffuse. By chemically cross-linking the solutions with glutaldehyde, the diffusion of nanoprobes becomes even slower. In gels, this behavior remains intriguing since the size of the nanoprobes is very small (~1.6 nm) and cross-linking does not affect small length scales ($\xi \sim 3–10$ nm).

Dehydration can cause significant changes in the gel structure, ranging from simple volumetric shrinking to cracking. We have designed, built, and tested an optical chamber appropriate for measuring the diffusion of fluorescent nanoprobes in gels and solutions as well as the volumetric changes of the dehydrating systems (see Fig.1). Here, we have used our microscope-based FCS setup to monitor and measure, simultaneously and continuously, in-situ changes of the fluorescence intensity as well as the concentration and diffusion time of the nanoprobe, TAMRA (see Figs. 4-6). Figure 4 shows that dehydration is slower in gels than in the corresponding solutions.

Acknowledgment: This work was supported by the Intramural Research Program of the *Eunice Kennedy Shriver* National Institute of Child Health and Human Development, NIH. H. Boukari acknowledges support from the National Science Foundation (NSF Grant #0630388), the National Aeronautics and Space Administration (NASA Grant #NNX09AU90A), and NIH-INBRE. We have benefitted greatly from discussions with Jack Douglas and Murugappan Muthukumar.

V. REFERENCES

[1] A.S. Hoffman, *Advanced Drug Delivery Reviews* **54**, 3 (2002).

[2] M. G. Cascone, L. Lazzeri, E. Sparvoli, M. Scatena, L.P. Serino, and S. Danti *Journal of Materials Science- Materials in Medicine 15*, 1309 (2004).

[3] N.A. Peppas and B. Kim *Journal of Drug Delivery Science and Technology* **2006**, *16*, 11 (2006).

[4] C. R. Nuttelman, S. M. Henry, K. S. Anseth, *Biomaterials* **23**, 3617 (2002).

[5] R. H. Schmedlen, K. S. Masters, J. L. West, *Biomaterials* **23**, 4325 (2002).

[6] A. Michelman-Ribeiro, H. Boukari, R. Nossal, F. Horkay *Macromolecules* **2004**, *37*, 10212.

[7] A. Michelman-Ribeiro, F. Horkay, R. Nossal, and H. Boukari, *Biomacrolecules* 8, 1595 (2007).

[8] D. Langevin and F. Rondelez *Polymer* **1978**, *19*,1875.

[9] De Gennes, P-G. *Scaling Concepts in Polymer Physics*; Cornell University Press; Ithaca, NY, 1979.

[10] M. Doi, S. F. Edwards *The Theory of Polymer Dynamics* (Clarendon; Oxford, U.K., 1986.)

[11] F. Horkay, A-M Hecht, S. Mallam, E. Geissler, and A. R. Rennie, *Macromolecules* **24**, 2896 (1991).

[12] F. Horkay, A-M. Hecht, E. Geissler *Macromolecules* **1994**, *27*, 1795.

[13] H. Boukari, C. Silva, R. Nossal, and F. Horkay, *Bioinspired Polymer Gels and Networks*, edited by F. Horkay, N.A. Langrana, A.J. Ryan, and J.D. Londono (Mater. Res. Soc. Symp. Proc. **1060E**, Warrendale, PA, 2008), 1060-LL07-03.

[14] http://www.gracebio.com/

[15] H. Boukari, R. Nossal, and D. L. Sackett, *Biochemistry* **42**, 1292 (2003).

[16] W. W. Webb *Appl*. *Opt*. **2001**, *40*, 3969.

[17] S. R. Aragon and R. Pecora *J*. *Chem*. *Phys*. **1976**, *64*, 1791.

[18] O. Krichevsky and G. Bonnet *Reports on Progress in Physics* **2002**, *65*, 251.

[19] Y. Chen, J. D. Müller, K. M. Berland, E. Gratton, *Methods* **19**, 234 (1999).

[20] M. A. Digman and E. Gratton, *Annu Rev Phys Chem*. **62**, 645-668 (2011).

[21] S. P. Zustiak, H. Boukari, and J. B. Leach, *Soft Matter* 6 3609-3618 (2010).

[22] S. P. Zustiak, J. Riley, H. Boukari, H. A. Gandjbakhche, R. Nossal, *Journal of Biomedical Optics* 17(12), 125004-125004 (2012).

[23] J. Lee, S. Masato, U. Kiminori and J. Mochida, *BMC Biotechnology*. **11**(1), 19 (2011).

[24] S. P. Zustiak, R. Nossal and D. L. Sackett, *Biophys J*. **101**(1), 255-264 (2011).

[25] T. Stylianopoulos, M. Z. Poh, N. Insin, M. G. Bawendi, D. Fukumura, L. L. Munn and R. K. Jain, *Biophys J*. **99**(5), 1342-1349 (2010).